

Proximity distance estimation based on electric field communication between 1 mm³ sensor nodes

Tatsuya Shinada¹ · Masanori Hashimoto¹ · Takao Onoye¹

Received: 31 March 2014 / Revised: 2 March 2015 / Accepted: 20 May 2015
© Springer Science+Business Media New York 2015

Abstract We are working toward actualizing a real-time 3D modeling system. This modeling system uses a sensor network that distributes many 1mm³-class sensor nodes in plastic clay. The distributed sensors sense the distances between them, and the sensor network collects the node-to-node distance information to recognize the clay shape by calculating the relative positions of the nodes. This paper proposes a distance estimation method based on electrical field communication through capacitive coupling between sensor nodes for the 3D modeling system. An electrical signal is transmitted through a closed loop composed of node-to-node capacitive coupling, and the signal attenuation is used for the distance estimation. We investigate the gain and directivity of the signal transmission with electric field and circuit simulations to explore appropriate electrode designs for the proposed method. We also evaluate the feasibility of the node localization with the proposed distance estimation method.

Keywords Proximity distance estimation · Capacitive coupling · Electric field communication · Electrode · Sensor node

1 Introduction

Services and applications using 3D models are becoming popular thanks to advances in information technology, and 3D computer graphics for entertainments and 3D CAD for architecture design, for example, are widely used. 3D

modeling software for PC is now commercially available. However, its usage is still not easy for most people. An intuitive and easy way of 3D modeling for non-expert people is demanded.

An approach for this purpose is that a person creates a physical shape with, for example, clay and captures its shape with a 3D scanner. An advantage of this approach is relatively easier its usage. However, it needs a certain amount of time before obtaining the shape on a computer since 3D scanning is not so fast. This could degrade the modeling efficiency since the turn-around-time between physical shape modification and reproduction on a computer is quite long. There are a few researches on tangible computer interfaces for 3D modeling, but they have not been put to practical use. For example, [1] embedded locators that used magnetic field for sensing in clay, but the size of the embedded locator was $7 \times 4 \times 2 \text{ cm}^3$ and hence the clay shape could not be well captured.

To enable intuitive real-time 3D modeling, we have devised a concept called “iClay” as illustrated in Fig. 1 and are working for its actualization. In this iClay system, a number of 1 mm³-class tiny sensor nodes are distributed in plastic clay and they organize a wireless sensor network. Each sensor node senses the distances to its adjacent nodes and this distance information is collected to a computer. The computer calculates the relative node positions and reproduces the 3D object based on the node-to-node distance information. 2D node localization is widely studied in sensor network area, and a few studies are also reported for 3D localization [2]. For eliminating battery exchange, each node is supposed to be powered through wireless power transmission, where the wireless power transmission for iClay system is under development. A preliminary experiment conducted by Akihara et al. demonstrated a wireless power transfer of 450 μW to a $2.5 \times 2.5 \text{ mm}^2$

✉ Masanori Hashimoto
hasimoto@ist.osaka-u.ac.jp

¹ Department of Information Systems Engineering,
Osaka University, Suita, Osaka, Japan

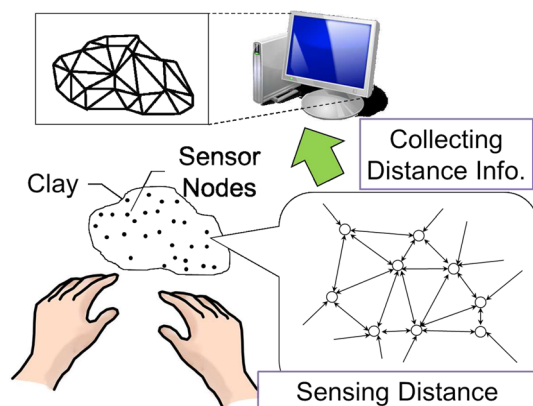


Fig. 1 iClay concept for real-time 3D shape acquisition

chip in which an on-chip inductor and a rectifier circuit were integrated [3]. The expected advantages of this approach are occlusion-free shape acquisition and real-time object reproduction, which cannot be achieved by the conventional approaches using a laser range finder or cameras.

This paper focuses on the sensor to sense the distances to its adjacent nodes and proposes a distance estimation method that uses electrical field communication through capacitive coupling between the nodes. We discuss its distance estimation accuracy assuming various electrode configurations through electro-magnetic and circuit simulations. In addition, we experimentally confirm that 3D node localization is possible even with the distance estimation error.

The rest of this paper is organized as follows. Section 2 describes the proposed distance estimation method. Section 3 shows experimental results to evaluate the electrode configuration. Supposing the distance estimation accuracy of the proposed method, a node localization experiment is performed in Sect. 4. Finally, Sect. 5 gives concluding remarks.

2 Proposed distance estimation method

In the iClay system, proximity sensing for all the directions in the clay is required for the embedded sensor nodes. Table 1 lists existing distance estimation methods. Time of arrival (TOA), time difference arrival (TDOA) and received signal strength indication (RSSI), which are often used in wireless sensor networks, are not capable of the mm-scale proximity sensing of interest due to a requirement of highly accurate time synchronization and the indistinguishable small attenuation in a short distance. Distance estimation methods based on light and ultrasonic are not suitable for a solid object in which obstacles

Table 1 Existing distance sensing methods

Method	Principle	Problem
Wireless TOA· TDOA	Prop. time	Proximity sensing difficult
Wireless RSSI	Attenuation	Proximity sensing difficult
Light	Reflection	Not propagate in clay
Ultrasonic	Reflection	Weak to obstacles
Eddy current	Mag. field	Strong directivity
Cap. coupling	Elec. field	Not studied enough

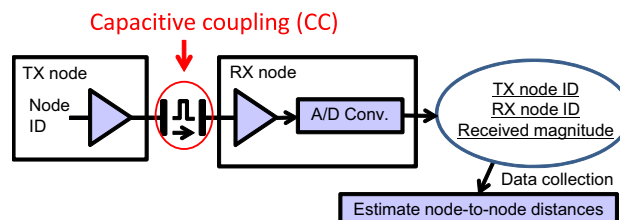


Fig. 2 Proposed distance estimation method

(nodes) are densely buried. Methods using eddy current and capacitive coupling could have a possibility to be used, but no proximity sensing methods readily applicable to iClay system are available, as far as the authors.

This paper proposes a distance sensing method that estimates the node-to-node distance based on the amplitude of a propagated signal through capacitive coupling between the sensor nodes. Figure 2 illustrates the overview of the proposed method. The TX (transmitter) node injects a pulse signal representing the TX node ID to the electrode of the TX node, the RX (receiver) node receives the signal, and its amplitude is digitized by an A/D converter. A set of data consisting of the TX node ID, the RX node ID and the digitized amplitude is delivered to a computer, and the computer estimates the node-to-node distance. The most significant feature of this method is that the amplitude changes in a short range since the capacitance value varies sensitively in such a proximity range. The solid object is not a problem for the proposed method. Another feature is that quasi-static electric field, which is used in the proposed method, tends to have a less directivity compared to magnetic field.

Communication using electrical field is widely studied for body area network (BAN) [4], which originates from personal area network (PAN) proposed by Zimmerman of IBM [5]. BAN is responsible for collecting personal biological information from sensors on and in the body, and the collected information is utilized for health management and care. BAN is largely classified into wireless body area network (WBAN), which uses electro-magnetic wave in UHF band, and intra-body communication (IBC), which

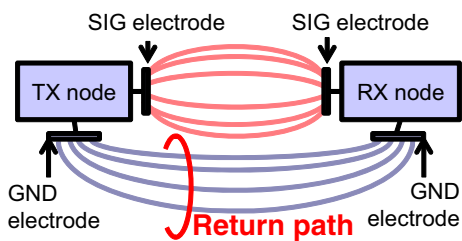


Fig. 3 Paired electrodes of SIG and GND for composing a closed loop

uses the human body as a signal transmission medium. The latter IBC has several advantages. For example, it has less interference with other electric devices since the signal is confined within the body. In addition, the usable frequency range is wider, and less power is consumed thanks to the less signal attenuation. IBC has two types; galvanic type and electric field type. The electric field type uses capacitive coupling between the node and the human body, which are called EF (electric field) communication.

In this EF communication, each of TX and RX has two electrodes of SIG and GND, and a loop path is organized consisting of the SIG electrode of TX, capacitive coupling, the body, capacitive coupling, the SIG electrode of RX, the GND electrode of RX, capacitive coupling, (earth, capacitive coupling) and the GND electrode of TX in this sequence. This loop is indispensable for signal transmission, since it is in quasi-static electrical field and the signal is not propagating as an electromagnetic wave. The proposed distance estimation method also uses EF communication, and hence the proposed node-to-node communication needs to construct a closed loop including a return path as shown in Fig. 3. For this purpose, each node should have two electrodes of SIG and GND within 1 mm³ volume. The following sections investigate the signal transmission characteristics with various configurations of the two electrodes, and evaluate the feasibility of iClay system through 3D node localization experiments taking into account the attainable accuracy of the proposed distance estimation method.

3 Experimental evaluation of electrode configuration

This section evaluates the characteristics of single-node-to-single-node communication through simulation.

3.1 Evaluation setup

Figure 4 shows the simulation overview. The simulation consisted of EF analysis for obtaining parasitic elements

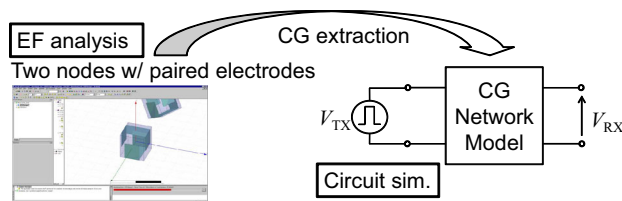


Fig. 4 Simulation overview

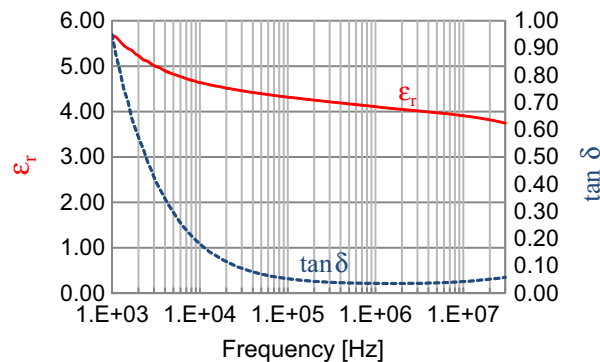


Fig. 5 Measured σ_r and $\tan \delta$ of resin clay

between the electrodes and pulse propagation analysis with circuit simulation. ANSYS Q3D extractor was used for the EF analysis, where Q3D can compute LCRG (inductance, capacitance, resistance and conductance) of parasitic elements by solving a model defined by structural and material information with boundary element method. In our EF analysis, C and G between the electrodes and CG between the electrode and the infinity point were extracted to compose a CG network model. Then, Synopsis HSPICE circuit simulator evaluated the output voltage using the CG network model in case that a pulse was injected.

As the characteristics of signal transmission, the directivity and gain were examined, where gain is defined as the ratio of output voltage V_{RX} to input voltage V_{TX} . The metric of directivity will be explained later. The higher gain contributes to power reduction and sensitivity improvement of the sensors, and the weak directivity is required for the distance estimation in all the directions. The weaker directivity improves the accuracy of the distance estimation.

We set relative dielectric constant (ϵ_r) and dielectric loss tangent ($\tan \delta$) of clay to 4.0 and 0.04. These numbers corresponds to the ϵ_r and $\tan \delta$ values of resin clay for 1 MHz sine wave, which are obtained from our measurement result shown in Fig. 5. This measurement was performed with Agilent E4294A impedance analyzer and Agilent 16451B dielectric test fixture. In the circuit simulation of Figure 4, the voltage source provided a 1 MHz square wave.

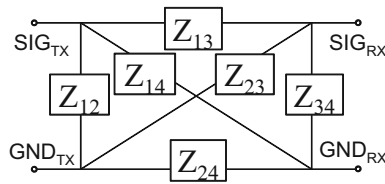


Fig. 6 Equivalent circuit for CG network model. Impedances to the infinity point are omitted

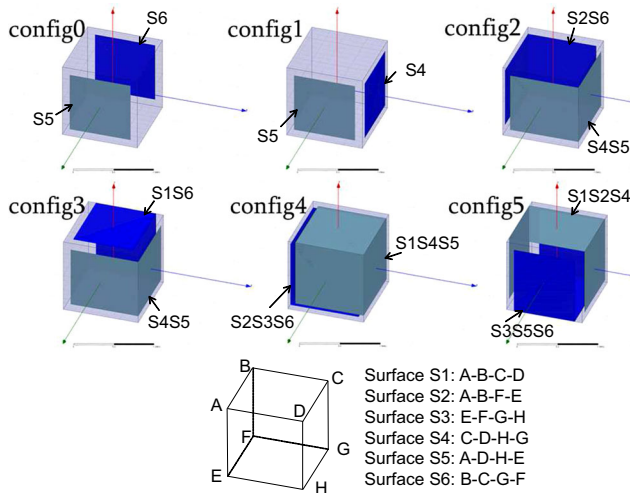


Fig. 7 A set of electrode configurations. For each configuration, the surface(s) of each electrode is annotated

Figure 6 represents an equivalent circuit of CG network model. This equivalent circuit omits the capacitances and conductances to the infinity point for simplifying the following discussion. It should be noted that the capacitances and conductances to the infinity point are considered in the circuit simulation. Supposing a voltage source whose amplitude is V_{TX} is connected between SIG_{TX} and GND_{TX} , V_{RX} , which is the voltage between SIG_{RX} and GND_{RX} , can be analytically derived by solving a closed circuit equation. Consequently, the gain $Ga(= V_{RX}/V_{TX})$ is expressed by

$$Ga = \frac{Z_{34}(Z_{14}Z_{23} - Z_{13}Z_{24})}{Z_{13}Z_{23}(Z_{14} + Z_{24}) + Z_{14}Z_{24}(Z_{13} + Z_{23}) + (Z_{13} + Z_{23})(Z_{14} + Z_{24})Z_{34}} \quad (1)$$

Equation (1) indicates that Ga is sensitive to Z_{34} between the SIG and GND electrodes at the RX node. In addition, when the symmetry between the SIG and GND electrodes deteriorates, the term of $Z_{14}Z_{23} - Z_{13}Z_{24}$ becomes smaller, which results in smaller Ga . Therefore, to maximize Ga , we should use the symmetric SIG and GND electrodes and

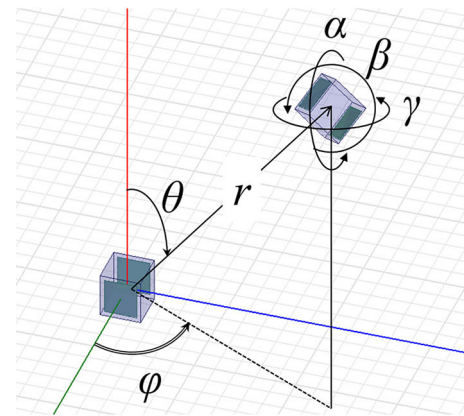


Fig. 8 Relative placement of TX and RX nodes

minimize the capacitance between these two electrodes. Taking into account these findings, we selected a set of electrode configurations shown in Fig. 7. The SIG and GND electrodes are put on the surfaces of the cube for maximizing the distance between them. In config 0 and 1, each electrode occupies a single face. Each electrode of config 2 and 3 uses two faces, and that of config 4 and 5 uses three faces.

Figure 8 illustrates the setup of the EF analysis. To evaluate the directivity of each electrode configuration, we fix a TX node at the center, and move and rotate the RX node for making a variety of their relative placements. The movement and rotation of the RX node are expressed by six parameters of (r, θ, ϕ) and (α, β, γ) . r is varied from 1.75 mm, which is the minimum distance for non-overlapping, to 10 mm, and $\theta, \phi, \alpha, \beta$ and γ are set to $n\pi/6 < 2\pi$ ($n = 1, 2, \dots$) independently.

Let us explain a metric for evaluating the directivity. The problem of the directivity is that it induces the uncertainty in V_{RX} and degrades the distance estimation accuracy. Here, this uncertainty in V_{RX} can be translated into the distance uncertainty (σ_r), which corresponds to the distance estimation error, as follows.

$$\sigma_r = \frac{\sigma_V}{dV_{RX}^{avg}/dr}, \quad (2)$$

where σ_V is the standard deviation of V_{RX} and V_{RX}^{avg} is the average of V_{RX} at each distance r for various sets of $\theta, \phi, \alpha, \beta$ and γ . This σ_r is used as the metric of the directivity and smaller σ_r is desirable. This equation tells us that the

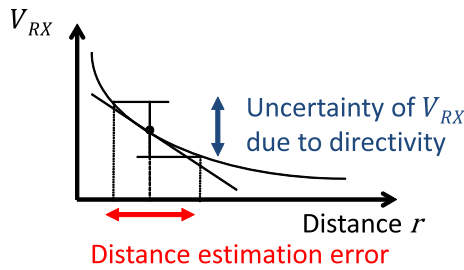


Fig. 9 Directivity induced uncertainty in V_{RX}

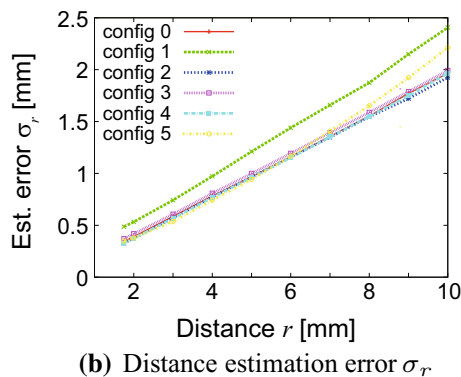
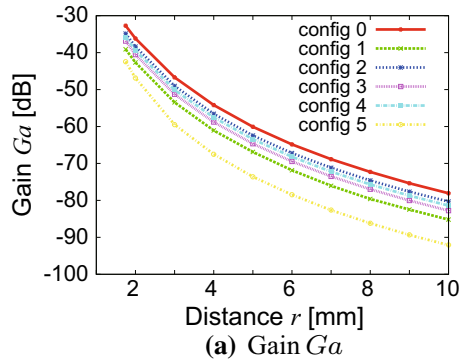


Fig. 10 Simulation results

distance estimation error becomes small when dV_{RX}^{avg}/dr is large (Fig. 9).

3.2 Experimental results

Simulation results of G_a and σ_r are shown in Fig. 10. It was observed that the received voltage, which corresponds to G_a for the fixed input voltage, was roughly proportional to $1/r^3$. Simpler face-to-face configurations of electrodes, such as config 0, 2, and 4, attained higher gain. In contrary, the gains of config 1, 3, and 5 decreased since the region where the two electrodes are adjacent becomes larger and then the capacitance between SIG and GND nodes becomes larger.

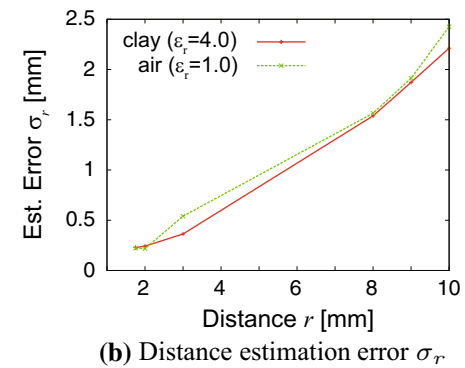
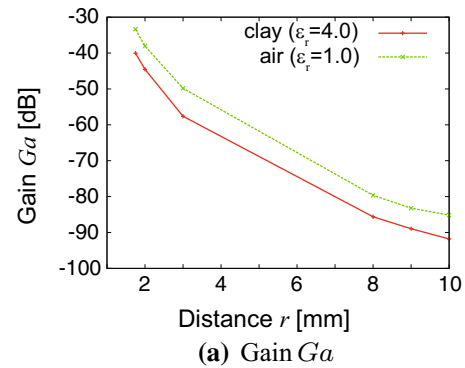


Fig. 11 Difference between two dielectric constants

On the other hand, the distance estimation error σ_r was similar for most of the configurations, while σ_r of config 1 was worse. Among them, config 2 achieved the smallest σ_r at the distance of 5 mm and above. In the short distance range of 3 and 4 mm, σ_r of config 5 was the smallest, while it increased more rapidly as r became larger. This tendency of config 5 was thought to originate from its lower gain. We thus improved the gain of config 5 in the following two ways; electrode size optimization and insertion of a material with lower dielectric constant.

As explained earlier with Eq. (1), the gain G_a is sensitive to the impedance between the SIG and GND electrodes Z_{34} , i.e. the capacitance between the SIG and GND electrodes in the same node. To reduce Z_{34} , i.e. the capacitance between the SIG and GND electrodes, inserting a material whose dielectric constant is low is effective. This approach can improve G_a without electrode modification. We evaluated the gain improvement by inserting air instead of clay into the sensor node, where the relative dielectric constant in the node was changed from 4.0 to 1.0. Figure 11(a) shows the gain difference between the two relative dielectric constants. As we expected, the lower relative dielectric constant of 1.0 achieved higher gain. However, the distance estimation error σ_r did not improve as shown in Fig. 11(b).

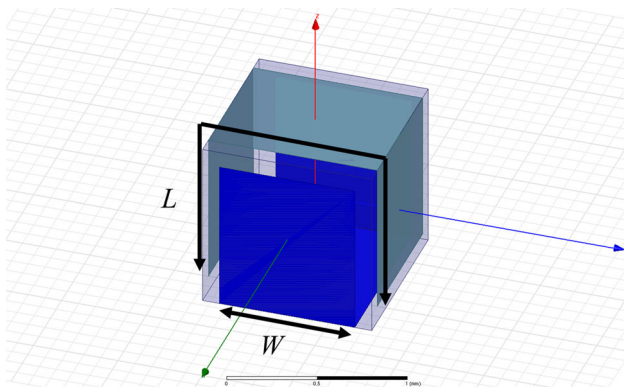


Fig. 12 Definition of W and L in config 5

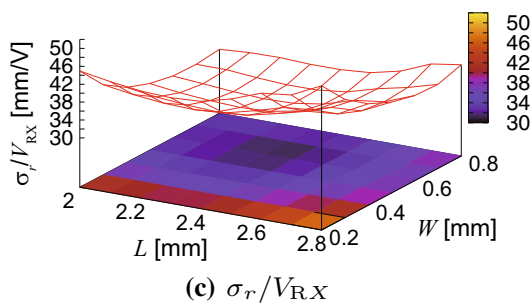
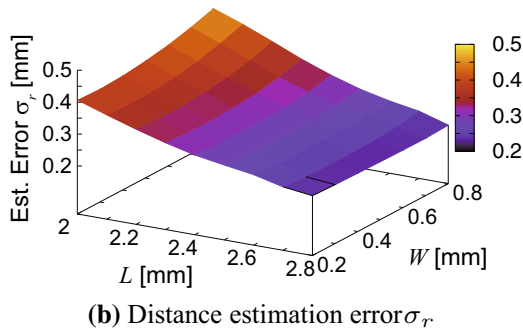
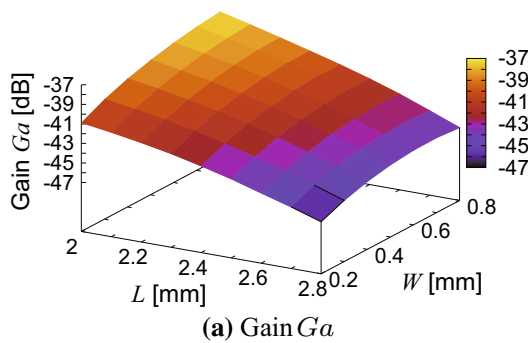


Fig. 13 Electrode size dependency ($r = 2.0$ mm)

We next evaluated G_a for various sizes of the electrodes while keeping the node volume 1 mm^3 . The electrode size affects the capacitance between the electrodes

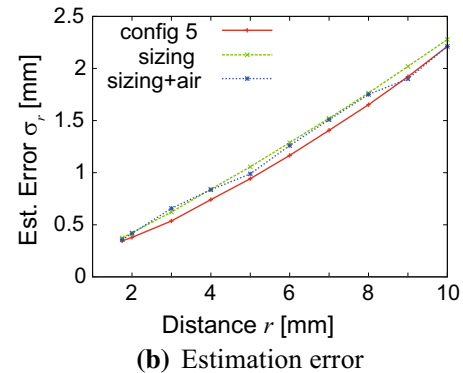
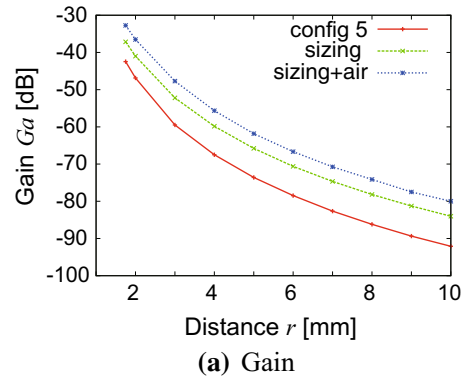


Fig. 14 Simulation results after electrode optimization

of different nodes, and hence G_a could be improved. Moreover, the electrode sizing changes the capacitance between the electrodes in the same node. The electrode size that makes the capacitance between the SIG and GND electrodes in the same node smaller might improve G_a . Figure 12 shows the definition of the electrode size parameters W and L in config 5. Figure 13 shows the evaluation result. The gain G_a improved as the length L became shorter and the width W narrower, which was due to the smaller capacitance between the SIG and GND electrodes in the same node. However, the distance estimation error σ_r also tended to become larger as L became shorter and W became narrower. The electrode sizing could not improve G_a and σ_r simultaneously. On the other hand, Fig. 13(a) shows a convex relation while Fig. 13(b) shows a concavo relation. We thus evaluated the electrode size that balanced gain and estimation error. We here sought for W and L that minimized σ_r/V_{RX} . Figure 13(c) shows σ_r/V_{RX} in W - L space. When the width W became narrower, G_a decreased while σ_r was roughly unchanged. Therefore, in this case, σ_r/V_{RX} degraded. On the other hand, σ_r/V_{RX} was less dependent on L , since the gain improvement and error degradation with shorter L canceled each other. In this evaluation, σ_r/V_{RX} became minimum when $W = 0.6$ mm and $L = 2.3$ mm.

We applied the lower dielectric constant of 1.0 and the electrode size optimized for σ_r/V_{RX} to config 5. The result is shown in Fig. 14. We can see that these were helpful to improve gain G_a . However, the distance estimation error σ_r did not improve, or rather degraded. This result suggests that the drastic estimation error reduction would be difficult to obtain.

4 Reproducing node positions

This section investigates the feasibility of node localization using the proposed distance estimation method. This experiment assumed that the distance estimation error of config 2 in Fig. 10 was expressed by

$$\sigma_r = 0.1932r - 0.0061 \text{ (mm)}. \tag{3}$$

The distance error was randomly given to each node-to-node pair assuming that the distance error followed a normal distribution whose standard deviation was σ_r .

We implemented a program that localized the nodes using the given node-to-node distance information. The procedure of this node localization program is shown in Fig. 15. This program first selects a robust set of five fully-

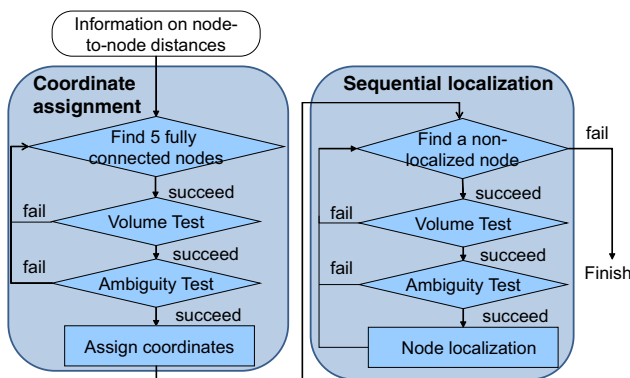


Fig. 15 Procedure of sequential node localization

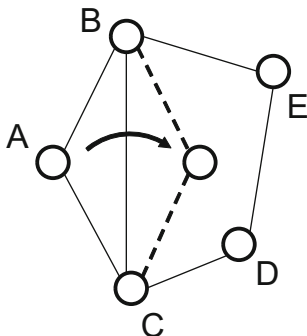


Fig. 16 Flip error. If A-D distance has large error, a flip may occur

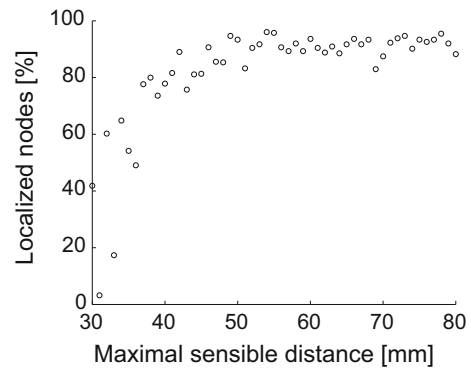


Fig. 17 Ratio of localized nodes

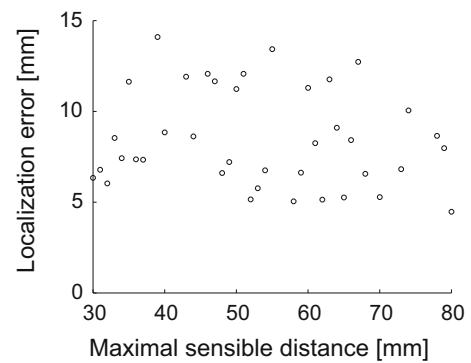


Fig. 18 Average localization error

connected nodes and assigns coordinates. After that, the nodes are sequentially localized one-by-one using the information of the nodes already localized. This sequential localization, however, has a problem. Once a flipping mistake happens due to indeterminacy (Fig. 16), it is likely that the nodes localized after this mistake have a larger localization error or localization itself becomes impossible. To minimize this problem, [2] proposes an approach that a robust set of nodes which are less likely to cause fatal mistakes are first searched, and they are used for node localization. This concept of robust node set is first proposed by Moore for 2D problem [6] and it is extended to 3D problem in [2]. To find a robust node set, volume test and ambiguity test are performed before the coordinate assignment and for each step of sequential node localization. Please see the details of these tests in [2].

The experiments of node localization were carried out for a $50 \times 50 \times 50 \text{ mm}^3$ clay in which 375 nodes were randomly distributed. This node density was selected according to a preliminary experiment that investigated the necessary node density for localization. The experimental results of node localization are shown in Figs. 17 and 18. The maximum sensible distance was changed in the experiments and it corresponds to the x-axis. The y-axis of

Fig. 17 represents the ratio of localized nodes. The y-axis of Fig. 18 is the average distance between the estimated position and the actual position.

This result shows that the 90 % nodes could be localized by using the proposed distance estimation method even though the distance estimation error of Eq. (3) existed as long as the maximum sensible distance was larger than 50 mm. The node localization became possible even with the shorter maximum sensible distance by increasing the node density. The average position error of over 5 mm was larger than our expectation. However, this number could happen even when the relative positions are reasonably reconstructed. This is because the origin is set by the first four nodes and the shift and rotation of the object easily increase this average localization error. Further investigation is necessary.

We finally carried out the node localization by changing the slope of Eq. (3). The result show that the node localization became impossible when the slope was larger than 0.2. This means that the distance estimation error of Eq. (3) is close to this upper boundary. Ideas to reduce the estimation error and to improve the localization accuracy are demanded.

5 Conclusion

This paper proposed a distance estimation method suitable for proximity region. The proposed method estimates the node-to-node distance according to the voltage magnitude of a signal propagated through capacitive coupling. The achievable distance estimation accuracy is experimentally evaluated with various configurations of paired electrodes. We also carried out node localization experiments with the error model of the proposed method, and showed that 90% of nodes could be localized. One of our future works is to detail the circuit implementation, such as the amplifier and A/D converter in the RX node and the driver in the TX node.

References

1. Reed, M. (2009) Prototyping digital clay as an active material. In: *Proceeding of the International Conference on Tangible and Embedded Interaction* (pp 339–342).
2. Mautz, R., Ochieng, W., Brodin, G., & Kemp, A. (2007). 3D wireless network localization from inconsistent distance observations. *Ad Hoc & Sensor Wireless Networks*, 3(2–3), 141–170.
3. Akihara, Y., Hirose, T., Tanaka, Y., Kuroki, N., Numa, M., & Hashimoto, M. Design of a wireless power transfer system for small-sized sensor devices. In: *Proceeding of the 28th Workshop on Circuits and Systems*, to appear.

4. Kohno, R., Hamaguchi, K., Li, H., & Takizawa, K. (2008). R & D and standardization of body area network (BAN) for medical healthcare. In: *Proceeding of the International Conference on Ultra-Wideband*, Vol. 3 (pp 5–8).
5. Zimmerman, T. G. (1996). Personal Area Networks: Near-Field Intrabody Communication. *IBM System Journal*, 35(3–4), 609–617.
6. Moore, D., Leonard, J., Rus, D., & Teller, S. (2004). Robust distributed network localization with noisy rangemeasurements. In: *Proceeding of the ACM Symposium on Networked Embedded Systems*.



Tatsuya Shinada received B.E. and M.E. degrees in Information Systems Engineering from Osaka University, Japan, in 2011 and 2013, respectively. His research interest includes electrical field communication and 3D localization.



Masanori Hashimoto received the B.E., M.E. and Ph.D. degrees in Communications and Computer Engineering from Kyoto University, Kyoto, Japan, in 1997, 1999, and 2001, respectively. Since 2004, he has been an Associate Professor in Department of Information Systems Engineering, Graduate School of Information Science and Technology, Osaka University. His research interest includes computer-aided design for digital integrated circuits, and high speed circuit design. Dr. Hashimoto served on the technical program committees for international conferences including DAC, ICCAD, ITC, Symposium on VLSI Circuits, ASP-DAC, DATE, ISPD and ICCD. He is a member of IEEE, ACM, IEICE and IPSJ.



Takao Onoye received the B.E. and M.E. degrees in Electronic Engineering, and Dr.Eng. degree in Information Systems Engineering all from Osaka University, Japan, in 1991, 1993, and 1997, respectively. He is currently a professor in the Department of Information Systems Engineering, Osaka University. His research interests include media-centric low-power architecture and its SoC implementation. He is a member of IEEE, IEICE, IPSJ, and ITE-J.